Symmetry breaking and self-trapping of a dipolar Bose-Einstein condensate in a double-well potential

Bo Xiong,[1,2] Jiangbin Gong,[3,2,4] Han Pu,[5] Weizhu Bao,[1,2] and Baowen Li[3,2,4]
[1]*Department of Mathematics, National University of Singapore, 117543, Singapore*
[2]*Centre of Computational Science and Engineering, National University of Singapore, 117542, Singapore*
[3]*Department of Physics, National University of Singapore, 117542, Singapore*
[4]*NUS Graduate School for Integrative Sciences and Engineering, 117597, Singapore*
[5]*Department of Physics and Astronomy, and Rice Quantum Institute, Rice University, Houston, Texas 77251-1892, USA*
(Received 17 November 2008; published 27 January 2009)

The quantum self-trapping phenomenon of a Bose-Einstein condensate (BEC) represents a remarkable nonlinear effect of wide interest. By considering a purely dipolar BEC in a double-well potential, we study how the dipole orientation affects the ground-state structure and the transition between self-trapping and Josephson oscillations in dynamics. Three-dimensional numerical results and an effective two-mode model demonstrate that the onset of self-trapping of a dipolar BEC can be radically modified by the dipole orientation. We also analyze the failure of the two-mode model in predicting the rate of Josephson oscillations. We hope that our results can motivate experimental work as well as future studies of self-trapping of ultracold dipolar gases in optical lattices.

DOI: 10.1103/PhysRevA.79.013626 PACS number(s): 03.75.Lm, 34.20.Cf, 32.10.Dk, 32.80.Qk

I. INTRODUCTION

Ultracold dipolar gases display a variety of unique properties that are absent in those dominated by *S*-wave scattering [1]. The successful Bose-Einstein condensation of ^{52}Cr atoms with a large magnetic dipole moment [2] and the first experimental realization of ultracold KRb polar molecular gas [3] are attracting even more experimental and theoretical interest in ultracold dipolar Bose-Einstein condensates (BECs). Other than possible applications in fields such as quantum information [4,5], one main motivation of studies of ultracold dipolar gases is to explore new physics afforded by the anisotropic and long-range dipole-dipole interaction. For a recent review, see Ref. [6]. Indeed, by varying the shape of a dipolar BEC, the dipole polarization axis, and the trapping geometry [7–9], the partially attractive and partially repulsive dipole-dipole interaction of a dipolar BEC can be easily manipulated to a great extent. Even more dramatically, by using the well-established Feshbach resonance technique [10–13], it is now possible to significantly reduce or completely shut off the effects of short-range interactions and hence realize purely dipolar gases, where the physics is completely dominated by the dipolar interaction. For example, superfluid transitions in purely dipolar Fermi gases [14,15], fractional quantum Hall states in purely dipolar gas trapped in a rotating optical lattice [16], and collapse features of a purely dipolar BEC [12] have been studied.

In this work, we investigate the properties of a dipolar BEC confined in a double-well potential. We focus on the structure of the ground-state wave function and the dynamical quantum self-trapping (QST) phenomenon which is among the most dramatic and counterintuitive effects induced by the self-interaction of a BEC. The QST phenomenon has been extensively studied in nondipolar BECs [17–19] and is closely connected with other physical contexts including the Josephson effect in superconductors [20] and the superfluidity of ^{4}He [21]. In particular, the QST of a nondipolar BEC in a double-well potential, which is sometimes called a Bose-Josephson junction, is now well understood [18,22–24] and has been observed experimentally [25]. From a time-independent point of view, on the mean-field level the self-interaction of a BEC can induce the emergence of stationary states with a large population imbalance between two wells. From a time-dependent point of view, the Josephson oscillation between the two wells can be suppressed by the self-interaction of a BEC, which can be regarded as a quantum Zeno effect because each atom in the BEC is being "measured" by all the other atoms.

Our interest here is how the anisotropic nature of the dipolar interaction can be exploited to manipulate the dipolar BEC in a double-well potential, as manifested in the static properties of the ground-state structure and in the dynamical evolution of the system prepared out of equilibrium. We approach this problem by three-dimensional numerical simulations. We find a wide region where the dynamics of a dipolar BEC can show either Josephson tunneling or QST without displaying signs of collapse. More significantly, we shall demonstrate that the dipole orientation can radically affect the transition from QST to Josephson oscillations. Furthermore, to gain more insight into the dynamical QST, we construct an effective two-mode model which has been widely applied in nondipolar systems. We find that this simple two-mode model successfully explains the numerically observed transition threshold between Josephson oscillations and QST, but fails to account for the oscillation frequency in the Josephson-oscillation regime. We provide a thorough analysis of the success and the failure of the two-mode model.

This paper is organized as follows. In Sec. II, after introducing a three-dimensional realistic model of a purely dipolar BEC trapped in a double-well potential, we study the structure of the ground-state wave function. In Sec. III, we present detailed simulation results regarding how the dipole orientation affects the self-trapping of the system. In Sec. IV, we attempt to use a simple effective two-mode model to

explain the dependence of the onset of self-trapping of a dipolar BEC upon the dipole orientation. In Sec. V, we discuss why our effective two-mode model cannot be used to estimate the oscillation frequency in the Josephson-oscillation regime. Section VI concludes and summarizes this work. The Appendix presents some details regarding our numerical calculations of the dipole-dipole interaction potential.

II. GROUND-STATE STRUCTURE

To be specific, let us consider a dipolar BEC of ^{52}Cr, which has a large magnetic moment $\mu=6\mu_B$ (μ_B is the Bohr magneton). We assume below that the S-wave scattering length is tuned to zero via the Feshbach resonance, thus resulting in a purely dipolar atomic BEC. We further assume that the system is confined in a trapping potential with a cylindrical symmetry in the x-y plane and a double-well structure along the z direction. That is, we consider a confining potential

$$V(x,y,z)=\frac{m}{2}(\omega_\rho^2x^2+\omega_\rho^2y^2+\omega_z^2z^2)+A\exp(-z^2/2\sigma_0^2),$$

where m is the atomic mass, $\omega_x=\omega_y=\omega_\rho$ is the confining harmonic frequency in the transverse direction, and ω_z is the confining harmonic frequency in the longitudinal direction, and A and σ_0 are the height and the width of a Gaussian profile modeling a barrier between the two potential wells along the z direction. Without loss of generality, we assume that the dipole moments are polarized by the external magnetic field and are confined in the x-z plane. The two-body dipolar interaction potential is then given by

$$U_{dd}(\mathbf{r})=d^2[r^2-3(z\cos\varphi+x\sin\varphi)^2]/r^5, \tag{1}$$

where φ is the angle between the polarized dipole orientation and the z axis, $d^2=\mu_0\mu^2/4\pi$, with μ_0 being the magnetic permeability of the vacuum. For convenience we define a dimensionless dipolar interaction parameter $D=(N-1)md^2/(\hbar^2a_{ho})$, where $a_{ho}=\sqrt{\hbar/(m\omega_z)}$ is the axial harmonic oscillator length and N is the total number of atoms. We can then adopt a unit system where the units for length, time, and energy are given by a_{ho}, $1/\omega_z$, and $\hbar\omega_z$, respectively. Unless specified otherwise, for the numerical results presented below we set $\omega_\rho/\omega_z=10$, $A=4\hbar\omega_z$, $\sigma_0=0.2a_{ho}$, and $D=0.6$ (which corresponds to about 2000 Cr atoms for the axial trapping frequency $\omega_z=2\pi\times330$ Hz). In such a confining potential, the mean-field dynamics of a purely dipolar BEC at $T=0$ is described by the following dimensionless time-dependent Gross-Pitaevskii equation:

$$i\frac{\partial\Psi(\mathbf{r},t)}{\partial t}=-\frac{1}{2}\nabla^2\Psi(\mathbf{r},t)+V(\mathbf{r})\Psi(\mathbf{r},t)+\int U_{dd}(\mathbf{r}-\mathbf{r}')|\Psi(\mathbf{r}',t)|^2\Psi(\mathbf{r},t)d^3\mathbf{r}', \tag{2}$$

where the macroscopic wave function Ψ is normalized to unity.

In our numerical simulations we adopt the time-splitting Fourier pseudospectral method [26,27]. The discretization

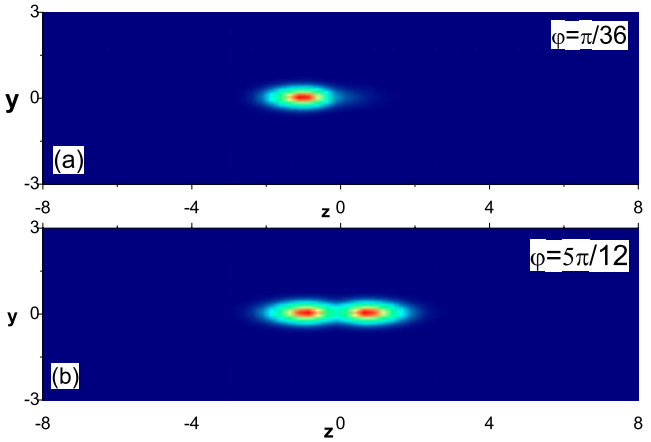

FIG. 1. (Color online) Column density of the ground-state density profile $\int|\Psi(\mathbf{r})|^2dx$ for two different angles φ.

used in our calculations is $\Delta t=0.005$ for time and $\Delta x=\Delta y=0.09375$, $\Delta z=0.25$ in space. The calculation is performed in a box of size (L_x,L_y,L_z). The values of L_x, L_y, and L_z are chosen such that the box is much larger than the size of the trapped condensate. We impose zero-boundary conditions for the wave-function amplitudes at $x=\pm L_x/2$, $y=\pm L_y/2$, and $z=\pm L_z/2$. Typically we set $L_x=L_y=6$, $L_z=16$. To evaluate the dipolar interaction potential that involves a convolution integral, we use the following fast-Fourier-transform technique:

$$\int U_{dd}(\mathbf{r}-\mathbf{r}')|\Psi(\mathbf{r}',t)|^2d^3\mathbf{r}'=F^{-1}\{F[U_{dd}(\mathbf{r})]F[|\Psi(\mathbf{r},t)|^2]\}, \tag{3}$$

where F and F^{-1} stand for fast Fourier transform and fast inverse Fourier transform, respectively. The term $F[U_{dd}(\mathbf{r})]$ in Eq. (3) is calculated analytically in momentum space (see details in the Appendix):

$$\begin{aligned}F[U_{dd}(\mathbf{r})]&=\int U_{dd}(\mathbf{r})e^{i\mathbf{k}\cdot\mathbf{r}}d^3\mathbf{r}\\&=\pi d^2[2\sin^2\varphi\sin^2\theta_{\mathbf{k}}\cos(2\phi_{\mathbf{k}})\\&\quad+2\sin(2\varphi)\sin(2\theta_{\mathbf{k}})\cos\phi_{\mathbf{k}}+(4/3-2\sin^2\varphi)\\&\quad\times(3\cos^2\theta_{\mathbf{k}}-1)],\end{aligned} \tag{4}$$

where $\theta_{\mathbf{k}}$ and $\phi_{\mathbf{k}}$ are the polar angle and the azimuthal angle in the spherical coordinate system for momentum space.

The ground state is obtained by evolving Eq. (2) in imaginary time. Figure 1 represents the ground-state wave functions for two different dipolar angles: $\varphi=\pi/36$ and $\varphi=5\pi/12$. One can clearly see that in the former case, the wave function is asymmetric and localized in one of the wells, while for the latter, the wave function is symmetric and the population is equally distributed in both wells. Given the geometry of the trapping potential, the effective dipolar interaction is predominantly attractive for small values of φ and repulsive for large values of φ. This explains the different structures of the ground-state wave function at different angles. Figure 2 shows the ground-state energy and chemical

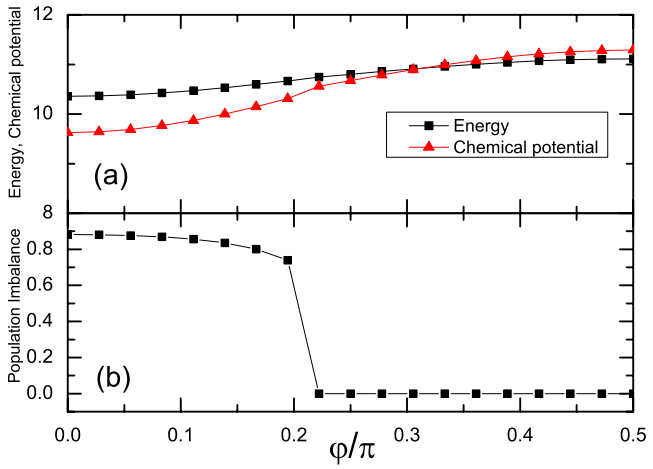

FIG. 2. (Color online) The ground-state energy and chemical potential as well as the population difference between the two wells as functions of φ.

potential as well as the population difference between the two wells as functions of φ. It indicates that the symmetric-asymmetric transition as induced by the variation of φ is a continuous one and the critical angle is about $\varphi=0.22\pi$.

III. SELF-TRAPPING AND JOSEPHSON OSCILLATIONS

We now turn to the dynamical properties of the system. We simulate the following situation. Initially we prepare the system in the ground state with $\varphi=\pi/36$. As shown in Fig. 1(a), for this dipole angle, the wave function is localized in one of the wells (for the example given, the atoms are localized in the left well). At $t=0$, we suddenly change φ to some other value and study the ensuing dynamics of the system.

In Fig. 3, we show the time evolution of $\Psi(\mathbf{r})$ for two different final values of the dipole orientation parameter φ. In Fig. 3(a), φ is chosen to be $\pi/4$ and the condensate is found to remain localized in the left well for all times even though the ground state for $\varphi=\pi/4$ should have population equally distributed in both wells [see Fig. 2(b)]. The system is hence clearly in the QST regime. By contrast, in the case of Fig. 3(b), φ is changed to $5\pi/12$ and the population exhibits regular oscillations. The system in this case is clearly in the Josephson-oscillation regime. Because the only parameter difference between Figs. 3(a) and 3(b) is the final value of φ, Fig. 3 vividly demonstrates the tunability of the system through the orientation of the dipoles, a feature obviously absent in nondipolar BEC's.

To examine in more detail how the dipole orientation impacts on the QST, we next scan the value of φ and then plot the corresponding time evolution of a normalized population imbalance S between the two wells: namely, the population difference divided by the total number of atoms. Results are shown in Fig. 4. It can be seen that there exists a critical angle $\varphi_c\approx 0.37\pi$: for $\varphi<\varphi_c$, the system is in the QST regime; for $\varphi>\varphi_c$, it enters the Josephson-oscillation regime. We have also checked the critical regime in more detail by scanning φ in smaller steps. In particular, we also show in

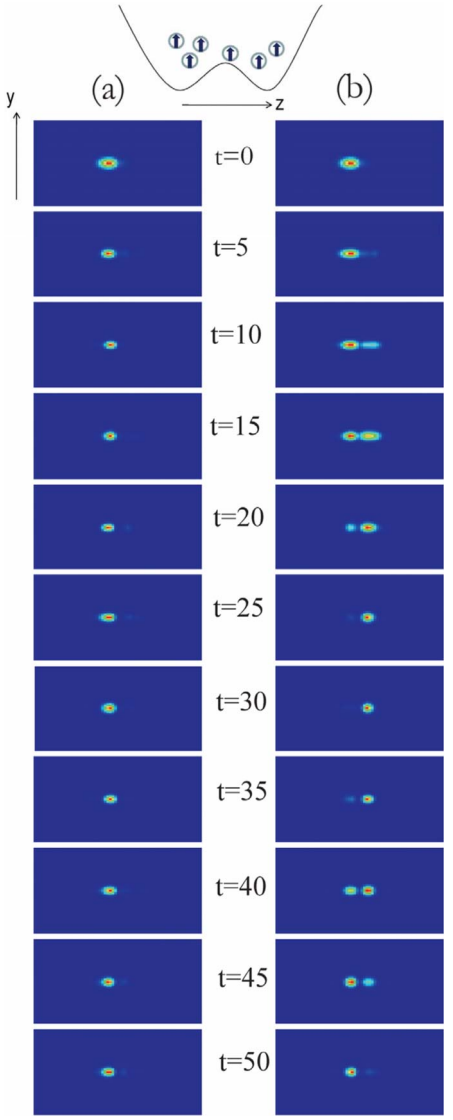

FIG. 3. (Color online) Column density of the condensate. (a) For the dipole orientation angle $\varphi=\pi/4$, the population is mainly trapped in the left well instead of tunneling between the two wells. (b) Changing only the dipole orientation parameter to $\varphi=5\pi/12$, the tunneling between the two wells, or the Josephson oscillation, is observed. See the text for other system parameters.

Fig. 4(a) the population dynamics for $\varphi=1353\pi/3600$, a value just above φ_c. Interestingly, the oscillation dynamics for that case shows noteworthy critical oscillation behavior. Evidently, then, our detailed results here further confirm that the dipole orientation of a dipolar BEC offers a simple and powerful means to manipulate the transition from QST to the Josephson oscillation.

We have also studied many cases with other trapping frequency ratios. For example, we let ω_ρ/ω_z vary from 10.0 to 5.0 via increasing ω_z. It is found that the frequency of the Josephson oscillation can be very sensitive to the trapping frequency ratio. For example, for $\omega_\rho/\omega_z=5.882$, $\varphi=5\pi/12$, and with the width of the initial wave-function in z narrowed by a factor of $\sqrt{10/5.882}$, the Josephson-oscillation frequency is more than 1.7 times larger than that shown in Fig.

4(a) for the same value of φ. If $\omega_\rho/\omega_z=5.882$ and if the width of the initial wave-function in z is not narrowed, then with all other parameters fixed, the condensate can already show clear signs of collapse (i.e., developing very high densities in our mean-field calculations) as we vary the dipole orientation. Interestingly, the condensate may collapse before we reach the critical point φ_c for the transition between QST and the Josephson oscillation. This being the case, a stable dipolar BEC in a double-well potential may be always in the QST regime.

IV. SIMPLE EFFECTIVE TWO-MODE MODEL

To understand and gain more insight into the dynamical behavior presented in the previous section, we now construct a two-mode model that has been widely used for the study of QST for nondipolar BECs. To that end we assume that the main feature of the time-evolving wave function $\Psi(\mathbf{r},t)$ is captured by two normalized real basis states:

$$\Psi(\mathbf{r},t) = \psi_1(t)\Phi_1(\mathbf{r}) + \psi_2(t)\Phi_2(\mathbf{r}), \tag{5}$$

where $\psi_{1,2}(t)=\sqrt{N_{1,2}(t)}e^{i\theta_{1,2}(t)}$ and $\Phi_{1,2}(r)$ are localized in each of the two wells. The total number of atoms is given by $|\psi_1|^2+|\psi_2|^2=N_T$. Substituting Eq. (5) into Eq. (2), we obtain

$$\begin{aligned} i\frac{d\psi_1(t)}{dt}\Phi_1(\mathbf{r}) + i\frac{d\psi_2(t)}{dt}\Phi_2(\mathbf{r}) = &-\frac{1}{2}[\psi_1(t)\nabla^2\Phi_1(\mathbf{r}) + \psi_2(t)\nabla^2\Phi_2(\mathbf{r})] + [\psi_1(t)V(\mathbf{r})\Phi_1(\mathbf{r}) + \psi_2(t)V(\mathbf{r})\Phi_2(\mathbf{r})] \\ &+ \left\{ |\psi_1|^2\psi_1\Phi_1(\mathbf{r}) \int U_{dd}(\mathbf{r}-\mathbf{r}')|\Phi_1(\mathbf{r}')|^2 d^3\mathbf{r}' + |\psi_1|^2\psi_2\left[\Phi_2(\mathbf{r}) \int U_{dd}(\mathbf{r}-\mathbf{r}')|\Phi_1(\mathbf{r}')|^2 d^3\mathbf{r}' \right.\right. \\ &\left. + \Phi_1(\mathbf{r}) \int U_{dd}(\mathbf{r}-\mathbf{r}')\Phi_1(\mathbf{r}')\Phi_2(\mathbf{r}')d^3\mathbf{r}' \right] + \psi_1^2\psi_2\Phi_1(\mathbf{r}) \int U_{dd}(\mathbf{r}-\mathbf{r}')\Phi_1(\mathbf{r}')\Phi_2(\mathbf{r}')d^3\mathbf{r}' \\ &+ \psi_1|\psi_2|^2\left[\Phi_2(\mathbf{r}) \int U_{dd}(\mathbf{r}-\mathbf{r}')\Phi_1(\mathbf{r}')\Phi_2(\mathbf{r}')d^3\mathbf{r}' + \Phi_1(\mathbf{r}) \int U_{dd}(\mathbf{r}-\mathbf{r}')|\Phi_2(\mathbf{r}')|^2 d^3\mathbf{r}' \right] \\ &\left. + \psi_1^*\psi_2^2\Phi_2(\mathbf{r}) \int U_{dd}(\mathbf{r}-\mathbf{r}')\Phi_1(\mathbf{r}')\Phi_2(\mathbf{r}')d^3\mathbf{r}' + |\psi_2|^2\psi_2\Phi_2(\mathbf{r}) \int U_{dd}(\mathbf{r}-\mathbf{r}')|\Phi_2(\mathbf{r}')|^2 d^3\mathbf{r}' \right\}. \end{aligned} \tag{6}$$

As in previous studies of QST of nondipolar BEC's, if we assume the overlap between the two modes being zero, namely,

$$\int \Phi_i(\mathbf{r})\Phi_j(\mathbf{r})d^3\mathbf{r} \approx \delta_{i,j}, \quad i,j=1,2,$$

$$\int f(\mathbf{r})\Phi_i(\mathbf{r})\Phi_j(\mathbf{r})d^3\mathbf{r} \approx 0, \quad i \neq j, \tag{7}$$

then most of the terms in Eq. (6) will vanish. Indeed, such a great simplification is the main advantage of a two-mode picture in the first place. Adopting this zero-overlap assumption, we obtain two simple coupled equations for $\psi_{1,2}(t)$:

$$i\frac{\partial\psi_1}{\partial t} = [(E_1^0 + B_{12}) + (A_{11} - B_{12})|\psi_1|^2]\psi_1 - \kappa\psi_2, \tag{8a}$$

$$i\frac{\partial\psi_2}{\partial t} = [(E_2^0 + B_{21}) + (A_{22} - B_{21})|\psi_2|^2]\psi_2 - \kappa\psi_1. \tag{8b}$$

The parameters in the above two-mode equations of motion are given by

$$E_i^0 = \int \frac{1}{2}[(\nabla\Phi_i)^2 + |\Phi_i(\mathbf{r})|^2 V(\mathbf{r})]d^3\mathbf{r}, \tag{9}$$

$$A_{ii} = \int U_{dd}(\mathbf{r}-\mathbf{r}')|\Phi_i(\mathbf{r})|^2|\Phi_i(\mathbf{r}')|^2 d^3\mathbf{r}d^3\mathbf{r}', \tag{10}$$

$$B_{12} = B_{21} = \int U_{dd}(\mathbf{r}-\mathbf{r}')|\Phi_1(\mathbf{r})|^2|\Phi_2(\mathbf{r}')|^2 d^3\mathbf{r}d^3\mathbf{r}', \tag{11}$$

$$\kappa \simeq -\int \left[\frac{1}{2}(\nabla\Phi_1 \cdot \nabla\Phi_2) + \Phi_1 V(\mathbf{r})\Phi_2 \right] d^3\mathbf{r}. \tag{12}$$

Here, A_{ii} and B_{12} are the "on-site" and "off-site" contributions of the dipolar interaction term, respectively. The presence of the off-site interaction term B_{12} is a unique feature for long-range interactions. $E_i^0+B_{12}$ can be regarded as an effective on-site energy for the two wells, and $A_{ii}-B_{12}$ can be regarded as an effective self-interaction strength, and κ is the coupling strength between the two modes and hence gives the characteristic rate of oscillations between the two modes

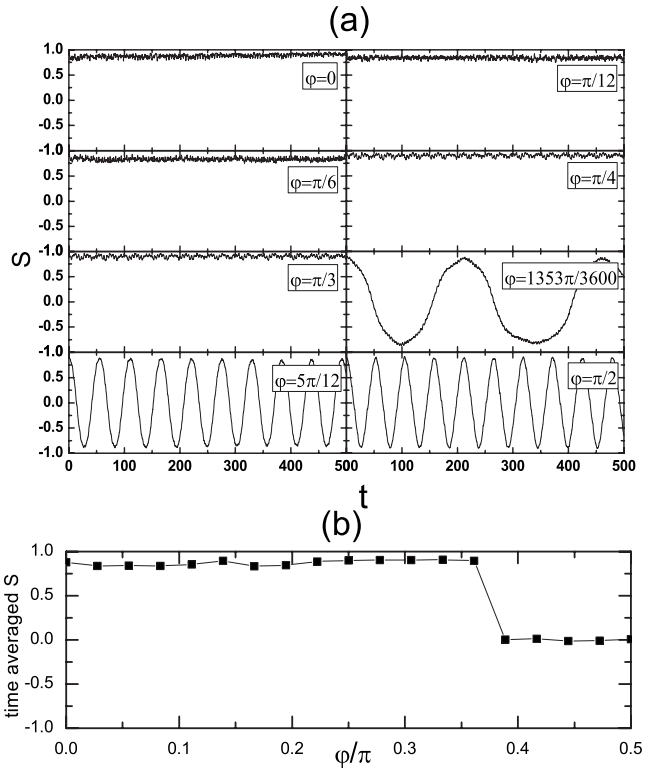

FIG. 4. (a) Population imbalance $S(t)$ versus time for different values of the dipole orientation parameter φ. As φ exceeds a critical value $\varphi_c \approx 0.37\pi$, the population imbalance starts to oscillate around zero. (b) Time-averaged $S(t)$ as a function of the dipole orientation parameter φ. When φ exceeds φ_c, the time-averaged population imbalance suddenly decreases to zero. The transition between Josephson oscillations and quantum self-trapping can hence be manipulated by tuning the dipole orientation. Other system parameters are the same as those used in Fig. 1.

if the nonlinear terms are neglected. Note that the expressions in Eq. (8) are very similar to those for a nondipolar BEC in a double-well potential [18] except that the off-site interaction term B_{12} is absent in nondipolar systems.

In terms of the population imbalance $S(t)=[|\psi_1(t)|^2 - |\psi_2(t)|^2]/N_T$ and a relative phase parameter $\phi(t) \equiv \theta_2(t) - \theta_1(t)$, Eqs. (8a) and (8b) assume an enlightening form

$$\dot{S}(t) = -\sqrt{1 - S^2(t)}\,\sin[\phi(t)], \tag{13a}$$

$$\dot{\phi}(t) = \Delta E + \Lambda S(t) + \frac{S(t)}{\sqrt{1 - S^2(t)}}\cos[\phi(t)], \tag{13b}$$

where the time variable is rescaled by a factor of 2κ, with the parameters ΔE and Λ defined by

$$\Delta E = \frac{E_1^0 - E_2^0}{2\kappa} + \frac{(A_{11} - A_{22})N_T}{4\kappa}, \tag{14a}$$

$$\Lambda = \frac{(A_{11} + A_{22} - 2B_{12})N_T}{4\kappa}. \tag{14b}$$

Because Eqs. (13a) and (13b) are exactly the same as those for a two-mode QST model of a nondipolar BEC, it is clear that within the above zero-overlap approximation, the underlying physics of the QST dynamics of a dipolar BEC should be similar to that of a nondipolar BEC. Indeed, the mechanical analog of Eqs. (13a) and (13b) is a classical nonrigid pendulum of tilt angle ϕ, angular momentum S, and a length proportional to $\sqrt{1-S^2(t)}$ [18]. For an initial condition $[S(0), \phi(0)]$, this pendulum will oscillate around $S=0$ if and only if $\Lambda < \Lambda_c$, where

$$\Lambda_c = \frac{2[1 - \Delta E S(0) + \sqrt{1 - S(0)^2}\cos\,\phi(0)]}{S(0)^2}. \tag{15}$$

Translating back to our BEC context, we have that if $\Lambda > \Lambda_c$, then the system will be in the QST regime, and if $\Lambda < \Lambda_c$, then Josephson oscillations can be expected.

The above two-mode analysis also indicates that the QST phenomenon of a dipolar BEC can be easily manipulated, because the important parameter Λ depends strongly on the dipole orientation as well as the trap geometry. Furthermore, the expression of Λ in Eq. (14b) implies that the competition between the on-site interaction terms A_{ii} and the off-site long-range term B_{12} might play a role in the QST physics. For example, if under some circumstances the on-site contribution cancels out the off-site contribution, then Λ will be small and hence QST will not occur.

Our discussions so far are based on the strong assumption that a two-mode model still applies well to a purely dipolar BEC in a three-dimensional potential with a double-well structure. However, because our simulations show that the density profile in each well depends strongly on the population imbalance, a simple two-mode model is not expected to work satisfactorily. As such, we propose an *effective* two-mode mode constructed in a self-consistent manner by first extracting useful information from our numerical simulations. Specifically, we use the normalized Gaussian ansatz

$$\Phi_i(\mathbf{r}) = \frac{e^{[-(x+x_i)^2/2a_i^2 - (y+y_i)^2/2b_i^2 - (z+z_i)^2/2c_i^2]}}{\sqrt{a_i b_i c_i}\,\pi^{3/4}} \tag{16}$$

to model the basis states $\Phi_{1,2}(\mathbf{r})$ in the two-mode model, with its parameters a_i, b_i, c_i, x_i, y_i, and z_i to be fitted by the long-time average properties of the density profile in our full three-dimensional simulations of Eq. (2). Once the parameters for the two basis states are obtained numerically, then the value of κ can be obtained analytically, and the values of A_{ii} and B_{12}, and hence the value of Λ, can all be obtained. In so doing, the location and width of the Gaussian ansatz for $\Phi_i(\mathbf{r})$ may change with the initial condition—e.g., the initial population imbalance. This feature is hence outside the conventional two-mode model of QST. For that reason our self-consistent effective two-mode model is expected to catch some features not available in a conventional two-mode model.

The results from our effective two-mode model are presented in Fig. 5. Figure 5(a) depicts how the values of the two-mode model parameters A_{11}, A_{22}, B_{12}, and κ change with the dipole orientation parameter φ. Figure 5(b) shows the φ dependence of Λ as well as Λ_c. From Fig. 5(b) it is seen that the value of Λ initially increases and then decreases to almost zero at about $\varphi \approx 0.37\pi$. On the other hand, the value

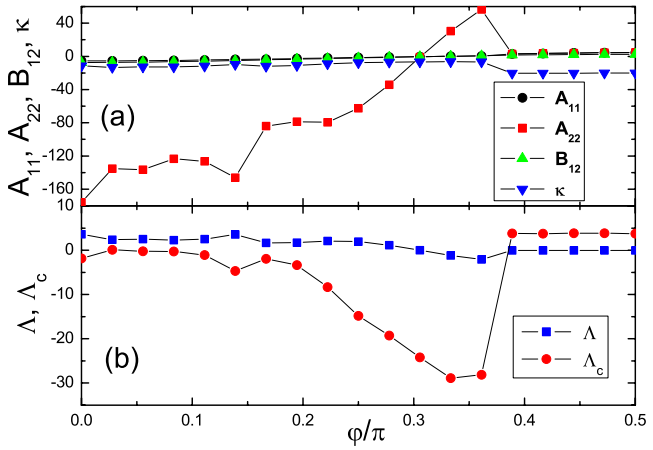

FIG. 5. (Color online) (a) Values for the two-mode model parameters A_{11}, A_{22}, B_{12}, and κ as functions of the dipolar orientation parameter φ, calculated by first fitting the Gaussian ansatz in (16) with the time-averaged properties of the density profile in our three-dimensional simulations. (b) Value of Λ calculated from Eq. (14b) and value of Λ_c calculated from Eq. (15) with $\phi(0)=0$ as a function of the dipolar orientation parameter φ. Note that for $\varphi<\varphi_c \approx 0.39\pi$, $\Lambda>\Lambda_c$, and for $\varphi>\varphi_c$, $\Lambda<\Lambda_c$.

of Λ_c, calculated from Eq. (15) with $\phi(0)=0$ (as an example), is seen to be less than Λ initially and then exceeds Λ at about $\varphi \approx 0.39\pi$. Therefore, as we tune the dipole orientation, our effective two-mode model displays a switch from $\Lambda>\Lambda_c$ to $\Lambda<\Lambda_c$, thereby predicting the transition from the self-trapping regime to the Josephson-oscillation regime at a critical value $\varphi \approx 0.39\pi$. The critical value obtained from the two-mode model matches with our previous numerical simulations of Eq. (2), where we observed $\varphi_c \approx 0.37\pi$. We conclude that at least in our effective two-mode model, the anisotropic nature of QST for a dipolar gas can be understood in terms of the φ dependence of the two-mode model parameters.

The results here indicate that when predicting the transition point between the QST regime and the Josephson-oscillation regime, the above-mentioned zero-overlap approximation is acceptable. But it should be noted that this zero-overlap approximation is a very rough one and there should be a high price for that. Indeed, as recently shown via a careful analysis of the validity of two-mode approximations for one-dimensional systems [28], the Josephson-oscillation rate based on a simple two-mode theory may differ greatly from the actual rate. With that in mind we ask if our effective two-mode picture can correctly describe other dynamical aspects. In particular, can our effective two-mode picture be employed to predict a right order of magnitude of the frequency of the regular Josephson oscillations seen in the four bottom panels in Fig. 4(a)? As it turns out, the answer is negative. For example, for $\varphi=\pi/2$, the oscillation period observed from Fig. 4(a) is about $t=50$, whereas the oscillation period from our effective two-mode model is about $\pi/\kappa \sim 0.157$ [see Eqs. (8a) and (8b)]. The difference is hence more than two orders of magnitude. Our next section is devoted to this interesting observation.

V. DISCUSSION

Here we provide a detailed analysis of the huge discrepancy between the two-mode parameter κ and the actual rate of the observed Josephson oscillations. Let us first reexamine the meaning of κ defined in Eq. (12). Clearly, for a three-dimensional problem, if the transverse direction is highly confined, the transverse motion will have a high kinetic energy and hence a large magnitude of wave-function gradients with respect to x and y. According to Eq. (12), this large transverse gradient will directly yield a large magnitude of κ. Hence, for tightly confined systems the magnitude of κ is largely contributed by the kinetic energy in the transverse direction. In our two-mode treatment, κ is identified as the parameter that determines the oscillation rate of the population between the two wells. As we show below, that κ differs significantly from the actual oscillation rate obtained numerically originates from the zero-overlap approximation made in the two-mode model.

Specifically, if we now drop the previous zero-overlap assumption, Eq. (6) leads to

$$i\frac{\partial \psi_1}{\partial t} = -\frac{\kappa C_{12} + E_1^0 + B_{12}}{C_{12}^2 - 1}\psi_1 + \frac{(E_2^0 + B_{21})C_{12} + \kappa}{C_{12}^2 - 1}\psi_2 + Q_1^{\mathrm{nl}}, \tag{17a}$$

$$i\frac{\partial \psi_2}{\partial t} = -\frac{\kappa C_{12} + E_2^0 + B_{21}}{C_{12}^2 - 1}\psi_2 + \frac{(E_1^0 + B_{12})C_{12} + \kappa}{C_{12}^2 - 1}\psi_1 + Q_2^{\mathrm{nl}}, \tag{17b}$$

where Q_1^{nl} and Q_2^{nl} are the nonlinear terms given by

$$Q_1^{\mathrm{nl}} \equiv \frac{C_{12}}{C_{12}^2 - 1}\sigma_2 - \frac{1}{C_{12}^2 - 1}\sigma_1,$$

$$Q_2^{\mathrm{nl}} \equiv \frac{C_{12}}{C_{12}^2 - 1}\sigma_1 - \frac{1}{C_{12}^2 - 1}\sigma_2, \tag{18}$$

with

$$\sigma_1 = (A_{11} - B_{12})|\psi_1|^2\psi_1 + 2D_{12}\psi_1^2\psi_2 + D_{12}|\psi_1|^2\psi_2^\star + G_{12}|\psi_2|^2\psi_1 + G_{12}\psi_1^\star\psi_2^2 + M_{12}|\psi_2|^2\psi_2, \tag{19a}$$

$$\sigma_2 = (A_{22} - B_{12})|\psi_2|^2\psi_2 + 2D_{21}\psi_2^2\psi_1 + D_{21}\psi_2^2\psi_1^\star + G_{21}|\psi_1|^2\psi_2 + G_{21}\psi_2^\star\psi_1^2 + M_{21}|\psi_1|^2\psi_1, \tag{19b}$$

and

$$C_{12} = \int \Phi_1(\mathbf{r})\Phi_2(\mathbf{r})d^3\mathbf{r},$$

$$D_{ij} = \int U_{dd}(\mathbf{r}-\mathbf{r}')\Phi_i(\mathbf{r})\Phi_j(\mathbf{r})|\Phi_i(\mathbf{r}')|^2 d^3\mathbf{r}\, d^3\mathbf{r}',$$

$$G_{ij} = \int U_{dd}(\mathbf{r}-\mathbf{r}')\Phi_i(\mathbf{r})\Phi_j(\mathbf{r})\Phi_i(\mathbf{r}')\Phi_j(\mathbf{r}')d^3\mathbf{r}\, d^3\mathbf{r}',$$

$$M_{ij} = \int U_{dd}(\mathbf{r}-\mathbf{r}')\Phi_i(\mathbf{r})\Phi_j(\mathbf{r})|\Phi_j(\mathbf{r}')|^2 d^3\mathbf{r}\, d^3\mathbf{r}'.$$

Evidently, then, once we drop the zero-overlap assumption, the two-mode treatment can no longer give a simple picture of the dynamics. Nevertheless, Eqs. (17a) and (17b) indicate that if we take into account the nonzero overlap C_{12}, the effective coupling between the two modes will be quite different. Indeed, if we assume that in the Josephson-oscillation regime the nonlinear terms $Q_1^{\rm nl}$ and $Q_2^{\rm nl}$ have a rather small impact on the oscillation rate, we have the corrected intermode coupling strength

$$\tilde{\kappa}_i = \frac{(E_i^0 + B_{12})C_{12} + \kappa}{C_{12}^2 - 1}. \tag{20}$$

As long as C_{ij} is nonzero, this corrected coupling strength $\tilde{\kappa}_i$ can differ significantly from κ. In particular, the kinetic energy in the transverse direction will make a positive contribution to $E_i^0 C_{12}$ but a negative contribution to κ. As a result, these two terms will largely cancel each other and hence the kinetic energy in the transverse direction will not directly enter into $\tilde{\kappa}_i$. For example, for the dipole orientation $\varphi = \pi/2$, using the same parameters as in our previous effective two-mode model, we obtain $\tilde{\kappa}_1 \approx \tilde{\kappa}_2 \approx -2.5$. One can then expect that the predicted Josephson-oscillation rate will be about one order of magnitude closer to our numerical value. Further taking into account the nonlinear terms $Q_i^{\rm nl}$, one can expect the magnitude of the intermode coupling to be further reduced and hence better agreement with simulation results can be obtained. For example, $Q_1^{\rm nl}$ contributes a term $-B_{12}|\psi_2|^2 C_{12}/(C_{12}^2-1)$ to the intermode coupling strength. This contribution will partially cancel the B_{12} term in $\tilde{\kappa}_1$ defined above. All these observations make it clear that the zero-overlap approximation is the main reason why our effective two-mode picture cannot be used to predict the rate of Josephson oscillations.

Consistent with our simulation result that the Josephson-oscillation rate depends strongly on the trapping geometry, we also find that if we slightly change the width of the fitting-mode wave functions $\Phi_{1,2}(\mathbf{r})$ and hence the value of C_{12}, then the value of $\tilde{\kappa}$ may also change significantly. This implies that if we take Eqs. (17a) and (17b) as an improved two-mode theory, then it is possible to refit the mode wave functions and obtain the right Josephson-oscillation rate. This approach is, however, not appealing to us, because by working with Eqs. (17a) and (17b) we lose the simplicity of a two-mode picture.

So why can our two-mode picture with the zero-overlap approximation still give the correct transition point between the QST regime and the Josephson-oscillation regime? The main reason lies in that our two-mode treatment already self-consistently used much information from the simulation results. In particular, in the QST regime, Λ_c defined in Eq. (15) is dominated by ΔE and hence scales with κ^{-1}, the same scaling behavior as Λ. As such, the actual magnitude of κ will not affect the ratio of Λ/Λ_c, the key index for a two-mode theory. In the Josephson-oscillation regime, $\Lambda_c \sim 1$ because $\Delta E \sim 0$ and $\Lambda \ll \Lambda_c$ because of the large magnitude of κ. This is also consistent with the condition for the Josephson-oscillation regime in the two-mode theory.

VI. CONCLUDING REMARKS

To conclude, using three-dimensional numerical simulations, we have investigated the structures of the ground state and the quantum self-trapping phenomenon of a purely dipolar Bose-Einstein condensate trapped in a double-well potential. The anisotropic nature of the dipole-dipole interaction is seen to impact dramatically the transition between two dynamical regimes: namely, the Josephson oscillation regime and the quantum self-trapping regime. This finding is the key result of this work.

To gain useful insights we constructed a simple effective two-mode model to understand the transition from the self-trapping regime to the Josephson-oscillation regime. Interestingly, though our two-mode picture is based on a rough zero-overlap approximation, the transition point obtained from our two-mode picture is in excellent agreement with our numerical simulations.

Somewhat expected, when it comes to the rate of the Josephson oscillations, our effective two-mode picture is no longer valid. We traced its failure to the zero-overlap approximation and discussed how we might be able to improve our effective two-mode treatment and find a better agreement with simulation results by lifting the zero-overlap approximation. However, by lifting the zero-overlap approximation, the simplicity of a two-mode picture in understanding the quantum self-trapping is lost.

There are now keen interest in the dynamics of BECs in optical lattices. In particular, the quantum self-trapping effect is known to play an important role in determining whether or not a condensate can spread out in an optical lattice [29]. The anisotropic nature of the quantum self-trapping of a dipolar BEC suggests that tuning the dipole orientation can lead to the control of the self-trapping effect in optical lattices and hence the control of transport properties of dipolar BECs in periodic potentials. We hope our work here may stimulate experimental efforts along this line.

ACKNOWLEDGMENTS

We thank Ryan Wilson for pointing out a missing factor of two in Eq. (4) in an earlier version of the manuscript. This work was supported in part by the Academic Research Fund (WBS Grant No. 158-000-002-112) (B.X., W.B., and B.L.), National University of Singapore and by the startup fund (WBS Grant No. R-144-050-193-101/133) as well as the "YIA" fund (WBS Grant No. R-144-000-195-123) (J.G.), National University of Singapore, and by the NSF and the Welch Foundation (Grant No. C-1669) (H.P.).

APPENDIX: FOURIER TRANSFORM OF THE DIPOLE-DIPOLE INTERACTION POTENTIAL

In this appendix we briefly outline how to use Fourier transformations to calculate the dipole-dipole interaction potential in our three-dimensional simulations. Assume that all the magnetic dipoles are aligned along an external magnetic field $\mathbf{B}(t)$, with

$$\mathbf{B}(t) = B[\hat{z}\cos\varphi + \sin\varphi(\hat{x}\cos\alpha + \hat{y}\sin\alpha)], \quad \text{(A1)}$$

where $\hat{x}$, $\hat{y}$, and $\hat{z}$ are units vectors in a Cartesian coordinate system. Then the dipole-dipole interaction energy becomes

$$\begin{aligned} U_{dd}(\mathbf{r}) &= d^2\frac{r^2 - 3[z\cos\varphi + \sin\varphi(x\cos\alpha + y\sin\alpha)]^2}{r^5} \\ &= -4\sqrt{\pi}\frac{d^2\sin^2\varphi\cos^2\alpha}{r^3}\left(Y_{00} - \sqrt{\frac{1}{5}}Y_{20}\right) \\ &\quad - i\sqrt{\frac{6\pi}{5}}\frac{d^2\sin^2\varphi\sin(2\alpha)}{r^3}(Y_{2-2} - Y_{22}) \\ &\quad - \sqrt{\frac{6\pi}{5}}\frac{d^2\sin 2\varphi\cos(\alpha)}{r^3}(Y_{2-1} - Y_{21}) \\ &\quad - i\sqrt{\frac{6\pi}{5}}\frac{d^2\sin 2\varphi\sin(\alpha)}{r^3}(Y_{2-1} + Y_{21}) \\ &\quad - 4\sqrt{\frac{\pi}{5}}\frac{d^2\cos^2\varphi}{r^3}Y_{20} + \frac{d^2\sin^2\varphi}{r^3}, \end{aligned} \quad \text{(A2)}$$

where Y_{lm} is the standard spherical harmonics. Consider then the Fourier transform of $U(\mathbf{r})$:

$$\tilde{U}_{dd}(\mathbf{k}) \equiv \int U_{dd}(\mathbf{r})e^{i\mathbf{k}\cdot\mathbf{r}}d^3\mathbf{r}. \quad \text{(A3)}$$

To evaluate this Fourier transform, we first use the identity

$$e^{i\mathbf{k}\cdot\mathbf{r}} = 4\pi\sum_{l=0}^{\infty}\sum_{m=-l}^{l} i^l Y_{lm}^*(\theta_\mathbf{k}, \phi_\mathbf{k}) j_l(kr) Y_{lm}(\theta, \phi), \quad \text{(A4)}$$

where $j_l(x)$ is the spherical Bessel function and $\theta_\mathbf{k}$ and $\phi_\mathbf{k}$ are two spherical angles that define the direction of the $\mathbf{k}$ vector. Upon integrations over the radial coordinate r, we finally have

$$\begin{aligned} \tilde{U}_{dd}(\mathbf{k}) = \pi d^2[&2\sin^2\varphi\sin^2\theta_\mathbf{k}\cos(2\phi_\mathbf{k} + 2\alpha) \\ &+ 2\sin 2\varphi\sin 2\theta_\mathbf{k}\cos(\phi_\mathbf{k} + \alpha) \\ &+ (4/3 - 2\sin^2\varphi)(3\cos^2\theta_\mathbf{k} - 1)]. \end{aligned} \quad \text{(A5)}$$

For our purpose here, for which the external magnetic field is time independent, we set $\alpha = 0$ and hence obtain Eq. (4).

[1] For example, H. Pu, W. Zhang, and P. Meystre, Phys. Rev. Lett. **87**, 140405 (2001); K. Góral, L. Santos, and M. Lewenstein, *ibid.* **88**, 170406 (2002); E. H. Rezayi, N. Read, and N. R. Cooper, *ibid.* **95**, 160404 (2005); S. Yi, L. You, and H. Pu, *ibid.* **93**, 040403 (2004); S. Yi and H. Pu, *ibid.* **97**, 020401 (2006); Y. Kawaguchi, H. Saito, and M. Ueda, *ibid.* **97**, 130404 (2006); D. H. J. O'Dell, S. Giovanazzi, and G. Kurizki, *ibid.* **90**, 110402 (2003); L. Santos, G. V. Shlyapnikov, and M. Lewenstein, *ibid.* **90**, 250403 (2003); S. Ronen, D. C. E. Bortolotti, and J. L. Bohn, *ibid.* **98**, 030406 (2007); O. Dutta and P. Meystre, *ibid.* **75**, 053604 (2007).

[2] A. Griesmaier, J. Werner, S. Hensler, J. Stuhler, and T. Pfau, Phys. Rev. Lett. **94**, 160401 (2005).

[3] K. K. Ni *et al.*, Science **322**, 231 (2008).

[4] D. DeMille, Phys. Rev. Lett. **88**, 067901 (2002).

[5] A. André *et al.*, Nat. Phys. **2**, 636 (2006).

[6] M. A. Baranov, Phys. Rep. **464**, 71 (2008).

[7] S. Yi and L. You, Phys. Rev. A **61**, 041604(R) (2000).

[8] K. Góral, K. Rzazewski, and T. Pfau, Phys. Rev. A **61**, 051601(R) (2000).

[9] L. Santos, G. V. Shlyapnikov, P. Zoller, and M. Lewenstein, Phys. Rev. Lett. **85**, 1791 (2000).

[10] J. Werner, A. Griesmaier, S. Hensler, J. Stuhler, T. Pfau, A. Simoni, and E. Tiesinga, Phys. Rev. Lett. **94**, 183201 (2005).

[11] T. Lahaye, *et al.*, Nature (London) **448**, 672 (2007).

[12] T. Lahaye, J. Metz, B. Frohlich, T. Koch, M. Meister, A. Griesmaier, T. Pfau, H. Saito, Y. Kawaguchi, and M. Ueda, Phys. Rev. Lett. **101**, 080401 (2008).

[13] T. Koch *et al.*, Nat. Phys. **4**, 218 (2008).

[14] M. A. Baranov, M. S. Marenko, V. S. Rychkov, and G. V. Shlyapnikov, Phys. Rev. A **66**, 013606 (2002).

[15] M. A. Baranov, L. Dobrek, and M. Lewenstein, Phys. Rev. Lett. **92**, 250403 (2004).

[16] M. A. Baranov, K. Osterloh, and M. Lewenstein, Phys. Rev. Lett. **94**, 070404 (2005).

[17] A. Aubry, S. Flach, K. Kladko, and E. Olbrich, Phys. Rev. Lett. **76**, 1607 (1996).

[18] A. Smerzi, S. Fantoni, S. Giovanazzi, and S. R. Shenoy, Phys. Rev. Lett. **79**, 4950 (1997).

[19] R. Gati and M. K. Oberthaler, J. Phys. B **40**, R61 (2007).

[20] B. D. Josephson, Phys. Lett. **1**, 251 (1962).

[21] P. W. Anderson, Rev. Mod. Phys. **38**, 298 (1966).

[22] S. Raghavan, A. Smerzi, S. Fantoni, and S. R. Shenoy, Phys. Rev. A **59**, 620 (1999).

[23] E. A. Ostrovskaya, Y. S. Kivshar, M. Lisak, B. Hall, F. Cattani, and D. Anderson, Phys. Rev. A **61**, 031601(R) (2000).

[24] L. Morales-Molina and J. B. Gong, Phys. Rev. A **78**, 041403(R) (2008).

[25] M. Albiez, R. Gati, J. Folling, S. Hunsmann, M. Cristiani, and M. K. Oberthaler, Phys. Rev. Lett. **95**, 010402 (2005).

[26] B. Fornberg, *A Practical Guide to Pseudospectral Methods* (Cambridge University Press, Cambridge, England, 1996).

[27] W. Bao, D. Jaksch, and P. A. Markowich, J. Comput. Phys. **187**, 318 (2003).

[28] D. Ananikian and T. Bergeman, Phys. Rev. A **73**, 013604 (2006).

[29] For example, M. Rosenkranz, D. Jaksch, F. Y. Lim, and W. Bao, Phys. Rev. A **77**, 063607 (2008).